

Superdeformed Band in ^{36}Ar Described by Projected Shell Model

Gui-Lu Long^{1,2} and Yang Sun^{1,3,4}

¹*Department of Physics, Tsinghua University, Beijing 100084, P.R. China*

²*Institute of Theoretical Physics, Chinese Academy of Sciences, Beijing 100080, P.R. China*

³*Department of Physics and Astronomy, University of Tennessee, Knoxville, Tennessee 37996*

⁴*Department of Physics, Xuzhou Normal University, Xuzhou, Jiangsu 221009, P.R. China*

The projected shell model implements shell model configuration mixing in the projected deformed basis. Our analysis on the recently observed superdeformed band in ^{36}Ar suggests that the neutron and proton 2-quasiparticle and the 4-quasiparticle bands cross the superdeformed ground band at the same angular momentum. This constitutes a picture of band disturbance in which the first and the second band-crossing, commonly seen at separate rotation frequencies in heavy nuclei, occur simultaneously. We also attempt to understand the assumptions of two previous theoretical calculations which interpreted this band. Electromagnetic properties of the band are predicted.

PACS: 21.10.Re, 21.60.Cs, 23.20.Lv, 27.30.+t

The topic of superdeformation has been at the forefront of nuclear structure physics since the observation of the first superdeformed (SD) band in ^{152}Dy [1]. Today, superdeformation at high spin is not an isolated phenomenon, but instead is observed across the nuclear periodic table [2], and its microscopic foundation has been firmly established. However, with the recent observation of the SD band in ^{36}Ar [3], it is astonishing that the quantum shell effects can stabilize the system at superdeformation in a nuclear system with such few particles (here $N = Z = 18$).

These new data have a large impact on theories, as they provide an ideal test case for nuclear structure models. The ^{36}Ar SD data presented in Ref. [3] were discussed by two theoretical calculations, the Cranked Nilsson-Strutinsky (CNS) model [4] and the spherical shell model (SM) [5]. The fact that these models can give a complementary description for the SD band in ^{36}Ar indicates that they both are appropriate approaches. Nevertheless, certain assumptions were made in both calculations. On the one hand, for a feasible SM calculation, the $1d_{5/2}$ orbital had to be excluded from the shell model space. It is known that in the deformed single-particle picture for the present SD minimum, the orbital $K = \frac{5}{2}$ of $1d_{5/2}$ lies very close to the Fermi levels, and it is expected that this orbital has strong correlation with other orbitals and contributes to the collective motion. It is therefore not obvious that excluding $1d_{5/2}$ is a proper approximation. On the other hand, no such exclusion is needed in the CNS calculations. However, pairing correlations were completely neglected in the CNS although there has been no indication that pairing plays a minor role in this nucleus.

The projected shell model (PSM) [6] is a shell model truncated in the Nilsson single-particle basis, with pairing correlation incorporated into the basis by a BCS calculation for the Nilsson states. More precisely, the truncation is first implemented in the multi-quasiparticle (qp) basis with respect to the deformed BCS vacuum $|0\rangle$ (see

Eq. (1) below); then the violation of rotational symmetry is removed by angular momentum projection [7] to form a shell model basis in the laboratory frame; finally a shell model Hamiltonian is diagonalized in this projected space. Thus, the PSM has the main advantages of mean-field theories because it can easily build in the model the most important nuclear correlations. It furthermore solves the problem fully quantum mechanically and provides a good approximation to the exact shell model solution. In fact, besides systematic reproductions of energy spectra and electromagnetic transitions in normally deformed nuclei [6], it has been shown that the SD bands in the $A \sim 190$ [8], $A \sim 130$ [9] and $A \sim 60$ [10] mass regions can be successfully described by the PSM.

It is clear that the PSM lies conceptually between the two approaches of the CNS and SM in [3]. In this paper, we use the PSM to analyze the new ^{36}Ar SD data and show that it gives comparable results to the SM in the spectrum calculation. The observed band disturbance in this SD band [3] can be understood in the PSM framework as simultaneous band-crossings among the SD ground band (g-band), 2-qp, and 4-qp bands at the same angular momentum. These 2- and 4-qp bands are based on the quasiparticles of the $1f_{7/2}$ subshell. Quantities such as $B(E2)$, g-factor, and pairing gap are also studied, to understand the assumptions in the CNS and SM calculations mentioned above.

In the present PSM calculation, particles in three major shells ($N = 1, 2, 3$) for both neutron and proton are activated so that the Fermi level lies roughly in the middle of the deformed single-particle states at deformation $\varepsilon_2 = 0.42$. The shell model space includes the 0-, 2- and 4-qp states:

$$|\phi\rangle_\kappa = \left\{ |0\rangle, \alpha_{n_i}^\dagger \alpha_{n_j}^\dagger |0\rangle, \alpha_{p_k}^\dagger \alpha_{p_l}^\dagger |0\rangle, \alpha_{n_i}^\dagger \alpha_{n_j}^\dagger \alpha_{p_k}^\dagger \alpha_{p_l}^\dagger |0\rangle \right\}, \quad (1)$$

where α^\dagger is the creation operator for a qp and the index n (p) denotes neutrons (protons). The projected

qp-vacuum $|0\rangle$ corresponds to the SD g-band, whereas the projected 2- and 4-qp states to 2- and 4-qp bands, respectively. The 2- and 4-qp states are selected so that the low-lying states for each kind of configuration should be included. If all multi-qp states were considered in Eq. (1), one would obtain the full shell model space generated by particles of the three major shells.

As in the usual PSM calculations, we employ the Hamiltonian [6]

$$\hat{H} = \hat{H}_0 - \frac{1}{2}\chi \sum_{\mu} \hat{Q}_{\mu}^{\dagger} \hat{Q}_{\mu} - G_M \hat{P}^{\dagger} \hat{P} - G_Q \sum_{\mu} \hat{P}_{\mu}^{\dagger} \hat{P}_{\mu}, \quad (2)$$

where \hat{H}_0 is the spherical single-particle Hamiltonian which contains a proper spin-orbit force, whose strengths (i.e. the Nilsson parameters κ and μ) are taken from Ref. [4]. The second term in the Hamiltonian is the Q-Q interaction and the last two terms are the monopole and quadrupole pairing interactions, respectively. The interaction strengths are determined as follows: the Q-Q interaction strength χ is adjusted by the self-consistent relation such that the input quadrupole deformation ε_2 and the one resulting from the HFB procedure coincide with each other [6]. The monopole pairing strength G_M is taken to be $G_M = [19.6 - 15.7(N - Z)/A]/A$ for neutrons and $G_M = 19.6/A$ for protons. This choice of G_M seems to be appropriate for the single-particle space employed in the present calculation in which the major shells $N = 1, 2, 3$ are included. Finally, the quadrupole pairing strength G_Q is assumed to be proportional to G_M , the proportionality constant being fixed to 0.20 in the present work.

The eigenvalue equation of the PSM for a given spin I takes the form [6]

$$\sum_{\kappa'} \{H_{\kappa\kappa'}^I - E^I N_{\kappa\kappa'}^I\} F_{\kappa'}^I = 0. \quad (3)$$

The expectation value of the Hamiltonian with respect to a “rotational band κ ” $H_{\kappa\kappa}^I/N_{\kappa\kappa}^I$ defines a band energy, and when plotted as functions of spin I , we call it a band diagram [6]. A band diagram displays bands of various configurations before they are mixed by the diagonalization procedure of Eq. (3). Irregularity in a spectrum may appear if a band is crossed by another one(s) at certain spin.

For the present problem, the eigenvalue equation is solved for different spins up to $I = 16$. This is the highest spin state of the SD band if the maximum spin contributed from the single particles is simply counted [3]. In the context of projection, spin distribution in each basis state of Eq. (1) is given by $\kappa \langle \phi | \hat{P}_{K_{\kappa}K_{\kappa}}^I | \phi \rangle_{\kappa}$ [11], where $\hat{P}_{K_{\kappa}K_{\kappa}}^I$ is the projection operator [7]. We have computed this quantity for each basis state and found that they approach zero for spins $I > 16$. In other words, one cannot find spin larger than 16 in the mean field states in

the present problem. This is band termination in the language of angular momentum projection.

Close to the neutron and proton Fermi levels of ^{36}Ar at deformation $\varepsilon_2 = 0.42$, there are four single-particle orbitals: $K = \frac{5}{2}$ of $1d_{5/2}$ and $K = \frac{1}{2}$ of $2s_{1/2}$ in the $N = 3$ shell, and $K = \frac{1}{2}$ and $\frac{3}{2}$ of $1f_{7/2}$ in the $N = 4$ shell. Thus, bands based on these orbitals are important for determining the high-spin properties of the low-lying states. In Fig. 1, the band diagram is shown. Different configurations are distinguished by different types of lines, and the filled circles represent the yrast states obtained after the configuration mixing. There are about 20 bands in the calculation, but only representative ones are displayed for discussion. Note that for the 2-qp bands, one curve represents two bands (a neutron band and a proton band) because they nearly coincide with each other for the entire spin region.

Among the 2-qp bands which start at energies of 5 – 6 MeV, one of them (dotted curve) consists of two $1f_{7/2}$ quasiparticles with $K = \frac{1}{2}$ and $\frac{3}{2}$ coupled to total $K = 1$. It shows a unique behavior as a function of spin. As spin increases, it goes down first but turns up at spin $I = 4$. This behavior has its origin in the spin alignment of a decoupled band as intensively discussed in Ref. [6]. Because of this, it can cross the g-band at about $I = 10$. On the other hand, there is another kind of 2-qp band (long-dashed curve, based on the coupling of $K = \frac{5}{2}$ of $1d_{5/2}$ and $K = \frac{1}{2}$ of $2s_{1/2}$) that shows a very different behavior: it goes up nearly parallel to the g-band, and has a very similar form as the g-band. This coupled band can never enter into the yrast region, thus playing a negligible role for the yrast band structure.

We have examined the other multi-qp states consisting of the $1d_{5/2}$ particles, such as the 2-qp state coupling $K = \frac{3}{2}$ and $\frac{5}{2}$ to $K = 1$. They lie in an even higher energy region, and have similar rotational behavior as the g-band. As far as the yrast energies are concerned, contributions of the $1d_{5/2}$ orbital to the spectrum calculations can therefore be renormalized. Influence of the $1d_{5/2}$ orbital on the absolute values of quadrupole moment can also be considered through the effective charges. This may have clarified the question of why the SM reproduced the data remarkably well even though it excluded the $1d_{5/2}$ orbital in the calculation [3].

The two decoupled ($K = 1$) 2-qp bands can be combined to a ($K = 2$) 4-qp band which represents simultaneously broken neutron and proton pairs. In Fig. 1, this 4-qp band (solid curve) also exhibits a decoupling behavior, and therefore, the 4-qp band can dive into the yrast region as well. It is interesting to see that bands from the three different configurations (0-, 2-, and 4-qp) cross at the same place near spin $I = 10$. This is in contrast to the common band-crossing picture leading to back-bendings in moment of inertia [7]. In the usual picture, one distinguishes two kinds of band-crossings: the first crossing

between the g-band and the 2-qp bands, and the second crossing between the 2-qp and the 4-qp bands. They cause the first and the second back-bending in moment of inertia, typically seen in the rare earth nuclei at spin $I \sim 12$ and ~ 24 , respectively [6]. The band-crossing picture in $N = Z$ nuclei in which a 4-qp band crosses directly with the g-band was suggested earlier by Sheikh *et al.* [12] and further elaborated in Ref. [13].

Thus, we can interpret the band disturbance in ^{36}Ar as a consequence of the simultaneous breaking of the $1f_{7/2}$ neutron and proton pairs. After the band-crossing, the main component of the yrast band is from the 4-qp band. We observe that all the (0-, 2-, and 4-qp) bands shown in Fig. 1 behave similarly at higher spins: above spin $I = 10$, all bands displayed are approximately parallel, indicating that they rotate with the same frequency.

In Fig. 2a, the PSM energy levels are compared with data, and with the SM calculations [3] in the $E(I) - E(I - 2)$ plot. We observe that the PSM can reasonably reproduce the data and the results are comparable with those of the SM. Following the SD band, one sees that the discontinuity around spin $I = 10$, which corresponds to the band-crossing discussed earlier, has been reproduced. Nevertheless, in contrast to near-perfect agreement at the low spins, the PSM calculation has small deviations from the data at the band-crossing region, and for the higher spin states. For the $N \sim Z$ nuclei, there has been an open question of whether the proton-neutron pair correlation plays a role in the structure discussions. It has been shown that with the renormalized pairing interactions of the like-nucleons in an effective Hamiltonian, one can account for the $T = 1$ part of the proton-neutron pairing [13]. However, whether the renormalization is sufficient for the complex region that exhibits the phenomenon of band-crossings, in particular when both neutron and proton pair alignments occur at the same time, is an interesting question to be investigated. We note also that the amount of angular momentum gained by the alignment is below what one expects from decoupled $f_{7/2}$ pairs. Experiment on the neighboring odd-mass nuclei may help us to understand this issue.

Fig. 2b and 2c present the calculated $B(\text{E}2)$ and g-factor values for the ^{36}Ar SD band. We found that the band-crossing does not cause sudden changes around the crossing spin in either quantity. In the $B(\text{E}2)$ calculations, the effective charges are 0.5e for neutrons and 1.5e for protons, which are the same as those used in previous work and in other shell models [14]. We emphasize that employment of different effective charges can modify the absolute $B(\text{E}2)$ values, but the essential spin dependence is determined by the wave functions. In Fig. 2b, the $B(\text{E}2)$ values begin to decrease after spin $I = 8$, and a smooth decrease is seen for higher spin states. At the band termination spin $I = 16$, an approximate 40% drop in $B(\text{E}2)$ (compared to the maximum value at $I = 8$) is

predicted. Our results thus suggest that a considerable collectivity remains even at the band termination. In the g-factor calculations, we use for g_l the free values and for g_s the free values damped by the usual 0.75 factor. The results are presented in Fig. 2c. We observe a smooth increase in the g-factor from 0.4 at the bandhead to $Z/A = 0.5$ at $I = 8$, and this rotor value remains thereafter. The nearly constant g-factor at higher spins indicates a cancellation between the proton and the neutron contribution. To see this clearly, we plot two additional curves in Fig. 2c where the neutron and proton contributions are separated. This is done by eliminating the proton (neutron) qp states in Eq. (1) in the calculation for neutron (proton) contribution. It is now seen that the proton alignment increases the g-factor, leading a peak at $I = 8$, whereas the neutron alignment decreases it, causing a valley at the same spin. The average of the two curves gives the total g-factor that shows a flat behavior as a function of spin. This reinforces our previous conclusion about the simultaneous breaking of the $1f_{7/2}$ neutron and proton pairs and their combined alignment. To test these predictions, lifetime measurements for the states in the ^{36}Ar SD band are required, and we hope that recently developed techniques [15] can permit the g-factor measurement.

We finally show the calculated pairing gaps in Fig. 2d, in which expectation values of the pair operator are calculated by using the PSM wave functions. It is found that for this lightest SD nucleus, both neutron and proton pairing gaps are larger than 1 MeV at $I = 0$, which is a non-negligible value that is of comparable size to pairing gaps in a heavy, deformed system. However, the pairing gaps fall quickly as the nucleus rotates. After $I = 8$, the falling continues, and saturates eventually at 0.3 – 0.4 MeV. This suggests that in order to describe the low-spin spectrum properly, pairing and its dynamic evolution are important. For the high spin states, the remaining weak pairing correlation may play a role in sustaining collectivity.

In summary, the new experimental data of the SD band in ^{36}Ar , the lightest SD nucleus reported so far, has been described by the PSM. The calculated energy levels agreed well with the data, as well as with the SM results. We may thus conclude that the PSM is an efficient shell model truncation scheme for the well-deformed light nuclei also, in which the quadrupole collectivity and pairing correlations dominate the properties. Similar conclusions have been drawn in the study of ^{48}Cr [14]. It has been found that in the present case, the 0-, 2-, and 4-qp bands cross each other at about spin $I = 10$. Therefore, the 2-qp configurations do not have a chance to play a major role in the structure of the SD yrast band because immediately after the band-crossing, the 4-qp band dominates the band structure. Analysis of the rotational behavior for various bands in the band diagram and calculation of the pairing gaps could help us understand the

assumptions in the CNS and the SM calculations that were previously used to interpret the data. Electromagnetic properties in this SD band have been studied with predictions made for the B(E2) and g-factor values.

Communication with Dr. C. Baktash is acknowledged. The authors sincerely thank Dr. D.J. Hartley for careful reading the manuscript. Y.S. thanks the Department of Physics of Tsinghua University for warm hospitality, and for support from its senior visiting scholar program. This work is supported also by the Major State Basic Research Developed Program Grant No. G2000077400, the China National Natural Science Foundation Grant No. 19775026, the Fok Ying Tung Education Foundation, and the Excellent Young University Teachers' Fund of Education Ministry of China.

- [1] P.J. Twin *et al.*, Phys. Rev. Lett. **57**, 811 (1986).
- [2] X.-L. Han and C.-L. Wu, At. Data Nucl. Data Tables **73**, 43 (1999); B. Singh, *et al.*, Nucl. Data Sheets, **78**, 1 (1996).
- [3] C.E. Svensson *et al.*, Phys. Rev. Lett. **85**, 2693 (2000).
- [4] T. Bengtsson and I. Ragnarsson, Nucl. Phys. **A436**, 14 (1985).
- [5] E. Caurier, A.P. Zuker, A. Poves and G. Martínez-Pinedo, Phys. Rev. **C50**, 225 (1994).
- [6] K. Hara and Y. Sun, Int. J. Mod. Phys. **E4**, 637 (1995).
- [7] P. Ring and P. Schuck, *The Nuclear Many Body Problem* (Springer-Verlag, New York, 1980).
- [8] Y. Sun, J.-y. Zhang and M. Guidry, Phys. Rev. Lett. **78**, 2321 (1997).
- [9] Y. Sun and M. Guidry, Phys. Rev. **C52**, R2844 (1995).
- [10] Y. Sun, J.-y. Zhang, M. Guidry and C.-L. Wu, Phys. Rev. Lett. **83**, 686 (1999).
- [11] K.H. Bhatt, S. Kahane and S. Raman, Phys. Rev. **C61**, 034317 (2000).
- [12] J.A. Sheikh, N. Rowley, M.A. Nagarajan and H.G. Price, Phys. Rev. Lett. **64**, 376 (1990).
- [13] S. Frauendorf and J.A. Sheikh, Nucl. Phys. **A645**, 509 (1999).
- [14] K. Hara, Y. Sun and T. Mizusaki, Phys. Rev. Lett. **83**, 1922 (1999).
- [15] R. Ernst *et al.*, Phys. Rev. Lett. **84**, 416 (2000).

FIG. 1. Band diagram (bands before configuration mixing) and the yrast band (the lowest band after configuration mixing, denoted by dots) for the superdeformed nucleus ^{36}Ar . Only the important lowest-lying bands in each configuration are shown.

FIG. 2. a) Transition energies $E(I) - E(I-2)$ along the superdeformed yrast band in ^{36}Ar (The experimental data and the SM results are taken from Ref. [3]); b) calculated B(E2) values; c) calculated g-factors; and d) calculated pairing gaps.

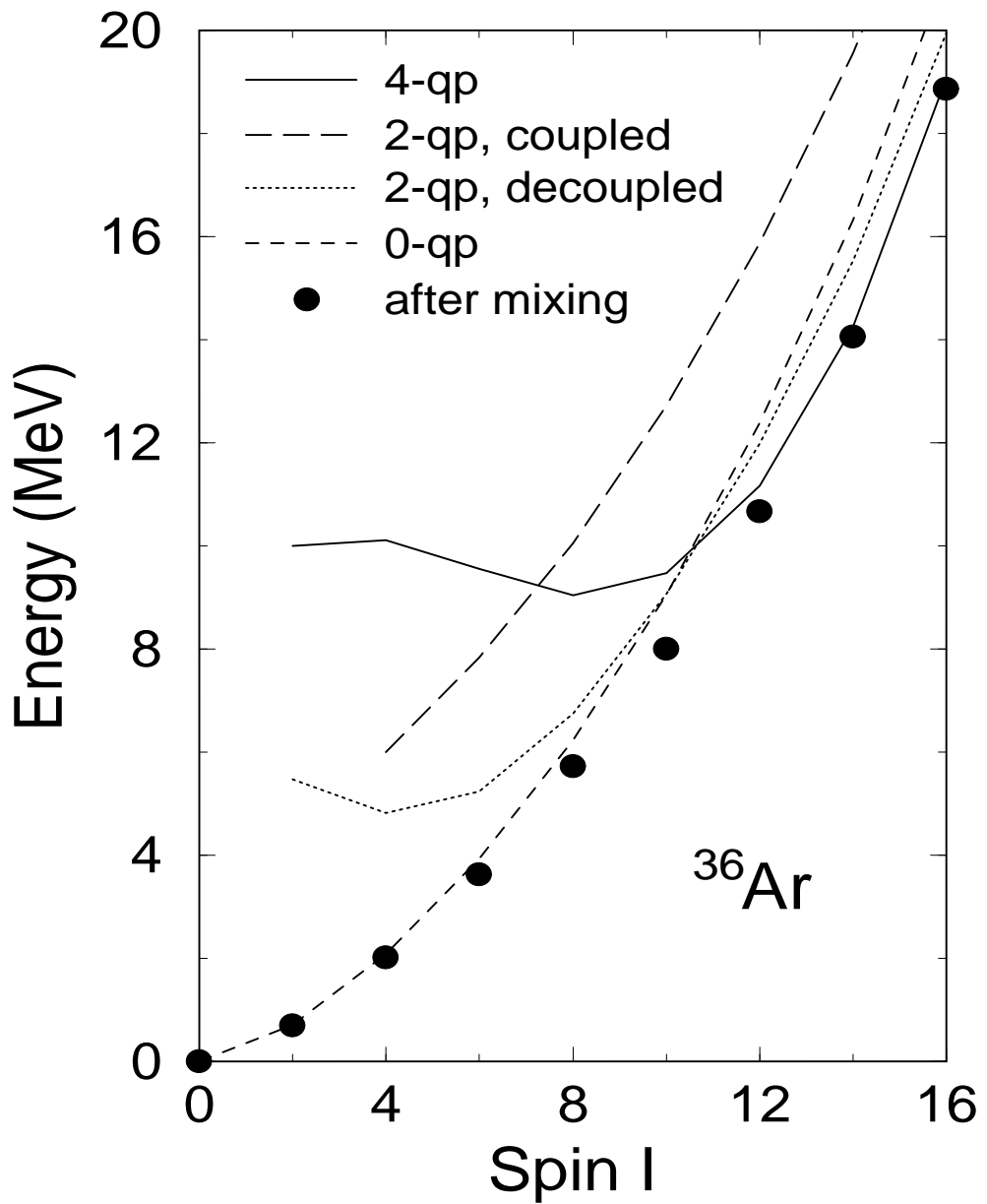


Fig.1, Long and Sun

Fig.2, Long and Sun

